

On the modeling of lattice thermal conductivity in semiconductor quantum dot superlattices

Alexander Khitun, Jianlin Liu, and Kang L. Wang

Citation: [Applied Physics Letters](#) **84**, 1762 (2004); doi: 10.1063/1.1668317

View online: <http://dx.doi.org/10.1063/1.1668317>

View Table of Contents: <http://scitation.aip.org/content/aip/journal/apl/84/10?ver=pdfcov>

Published by the [AIP Publishing](#)

Articles you may be interested in

[Strong reduction of the lattice thermal conductivity in superlattices and quantum dot superlattices](#)

AIP Conf. Proc. **1449**, 33 (2012); 10.1063/1.4731490

[Thermal conductivity of Si/SiGe superlattice films](#)

J. Appl. Phys. **104**, 114301 (2008); 10.1063/1.3032602

[Thermal conductivity of Si/SiGe superlattice nanowires](#)

Appl. Phys. Lett. **83**, 3186 (2003); 10.1063/1.1619221

[Thermal conductivity of Si/SiGe and SiGe/SiGe superlattices](#)

Appl. Phys. Lett. **80**, 1737 (2002); 10.1063/1.1455693

[In-plane lattice thermal conductivity of a quantum-dot superlattice](#)

J. Appl. Phys. **88**, 696 (2000); 10.1063/1.373723

A promotional banner for Applied Physics Reviews. On the left is a thumbnail image of a journal cover for 'AIP Applied Physics Reviews' featuring a diagram of a quantum device. The main part of the banner has a blue background with a molecular structure. The text 'NEW Special Topic Sections' is prominently displayed in white. Below this, on an orange background, it says 'NOW ONLINE' in yellow, followed by 'Lithium Niobate Properties and Applications: Reviews of Emerging Trends' in white. The AIP Applied Physics Reviews logo is in the bottom right corner.

NEW Special Topic Sections

NOW ONLINE
Lithium Niobate Properties and Applications:
Reviews of Emerging Trends

AIP Applied Physics Reviews

On the modeling of lattice thermal conductivity in semiconductor quantum dot superlattices

Alexander Khitun^{a)}

Device Research Laboratory, Department of Electrical Engineering, University of California at Los Angeles, Los Angeles, California 90095-1594

Jianlin Liu

Department of Electrical Engineering, University of California at Riverside, Riverside, California 92521

Kang L. Wang

Device Research Laboratory, Department of Electrical Engineering, University of California at Los Angeles, Los Angeles, California 90095-1594

(Received 18 August 2003; accepted 14 January 2004)

We present a theoretical model for the cross-plane lattice thermal conductivity calculations in semiconductor quantum dot superlattices. Based on continuum approximation, our model takes into account scattering of acoustic phonons on quantum dots. In most practical cases, the dot volume fraction is relatively small and/or dot and host materials have a small acoustic mismatch. This fact lets us take into account only first order scattering events and to significantly simplify the calculations. The results of numerical simulations carried out for Si/Ge quantum dot superlattices show good agreement with experimental data. The proposed model is useful for many applications recently suggested for semiconductor quantum-dot superlattices. © 2004 American Institute of Physics. [DOI: 10.1063/1.1668317]

For the past two decades, semiconductor quantum dot superlattices (QDS) attract growing interest due to the opportunity to engineer its electronic properties.^{1,2} Until recently, most attention has been focused on possible electronics and optoelectronics applications.^{3,4} Recently, there is increased interest in studying thermal properties in QDS. An intriguing ability of independent control of electronic and thermal properties in QDS stimulated a great deal of interests devoted mainly to possible thermoelectric applications.⁵ An increase in thermoelectric figure of merit in QDS is anticipated due to the modification of its thermal properties in addition to electronic ones.⁶ All of this motivates current interest in understanding and modeling QDS thermal properties. As bulk of heat in semiconductors is transported by lattice vibrations, theoretical efforts are focused on the lattice thermal transport. Rigorous solutions of the problem by direct molecular dynamic (MD) techniques⁷ may be possible in the future with increased computation power. To date, one must use approximated models to evaluate lattice thermal conductivity, taking into account specific properties of QDS, such as structure and composition.

In this letter, we report a theoretical model of cross-plane lattice thermal conductivity of semiconductor QDS, applicable for most grown superlattices reported in the literature.^{8–10}

In the relaxation-time approximation the expression for the lattice thermal conductivity can be written in an integral form as¹¹

$$\kappa = \frac{1}{3} \int S(\omega) \nu_g l(\omega) d\omega, \quad (1)$$

where $S(\omega)$ is the contribution to the specific heat per frequency interval from lattice wave of frequency ω , ν_g is the phonon group velocity, and $l(\omega)$ is the phonon mean-free-path. Thermal conductivity arises from phonon relaxation in different scattering processes, which do not conserve crystal momentum.¹¹ The mean-free-path $l(\omega)$ is used to represent the combined effect of these processes

$$\frac{1}{l(\omega)} = \frac{1}{l_P(\omega)} + \frac{1}{l_I(\omega)} + \frac{1}{l_B(\omega)} + \dots, \quad (2)$$

where the first three terms are the most important lengths associated with the Umklapp, phonon-impurity atoms, and phonon-boundary scattering mechanisms, respectively. The calculation procedures for the above processes are known and can be found elsewhere.^{11,12}

In order to construct a theoretical formalism for QDS, we have to take into account a new phonon scattering process—scattering on quantum dots. Thus, we must calculate one more phonon attenuation length $l_D(\omega) = V/\sigma_V$ (where σ_V is the total phonon scattering cross section in volume V) and to add it to the sum in Eq. (2).

As the characteristic size of quantum dots in a superlattice exceeds hundred of nanometers (typically quantum dots grown in Stranski–Krastanov mode have about 100 nm in base and 10 nm in height) and thus, each dot may consist of more than 10^5 atoms. Since the scale of our interest is much higher than the inter atom distance, we can apply the continuum model approximation and treat quantum dots as regions having the density and the sound velocity different from those in the host matrix (see Fig. 1). Due to the mismatch of the acoustic properties, the dots act as scatters to the propagating lattice waves.

^{a)}Electronic mail: ahit@ee.ucla.edu

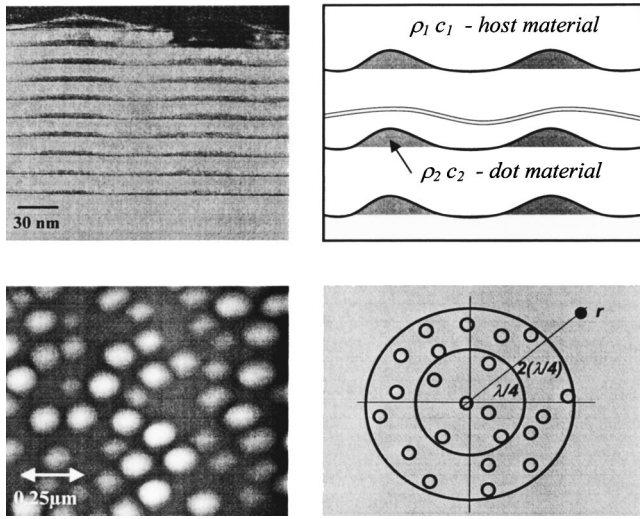


FIG. 1. Quantum dot structure used in simulations. On the left-hand side there are the cross-plane TEM image and the top view AFM image of the Si/Ge QDS. The darker regions in TEM image correspond to Ge, while lighter regions in AFM depict Ge quantum dots. On the right-hand side there are model pictures used in calculations. The superlattice is treated as a structure having regions of different acoustic properties (ρ is the density and c is the sound velocity). The scattering from each quantum dot layer is obtained by integration over the half-period zones. The scattering from all scatters in a given zone is on average equal in magnitude but opposite in sign from the contribution of the preceeding zone.

The problem of elastic wave propagation in a media containing multiple scatters is known from acoustics and will not be reproduced here. Following the general approach,^{13–15} the solution of the wave equation at any point r can be found as a sum of the incident ψ_0 and scattered ψ_s waves $\psi(r) = \psi^{\text{in}}(r) + \psi^s(r)$, where $\psi^{\text{in}}(r) = \exp(ikr)$ and

$$\psi^s(r) = \sum_j \psi^s(r|r_j),$$

summing through all scattered waves. Taking into account the specific scatter arrangement within spatially ordered layers (Fig. 1), the total scattered field in QDS is found by summation of scattered waves from all layers.

In order to find the scattered field produced by a single layer, we apply the generalized result of a classical scattering theory, the so-called optical theorem¹⁶ which gives us the expression for the total scattering cross section of one layer with spatially random distributed scatters as follows:

$$\sigma(k_i) = -\text{Im}\langle f(k_i, k_i) \rangle / k_0, \quad (3)$$

where k_i defines the direction of wave propagation, $\langle f(k_i, k_i) \rangle$ is the forward scattering amplitude and k_0 is the wave number where $|k_i| = k_0$. The angular brackets in Eq. (3) denote the averaging over the ensemble. Our special interest is devoted to the *weak scattering density* limit $|nf(k_i, k_i)/k_0^2| \ll 1$, where $f(k_i, k_i)$ is the scattering amplitude of a single scatter, and n is the scatter density. For many semiconductor materials, for example, Si and Ge, this limit takes place in most cases due to the relatively low quantum dot volume fraction ($5\% \leq$) and the finite acoustic mismatch between the host and dot materials ($\chi = 0.78$). In this particular case, the interaction between different scatters can be estimated by using the *multiple forward scattering approximation* (MFSA).¹⁷

To find the total forward scattering produced by the ensemble, only forward scattering from single scatters should be taken into account while the effect of backward scattering is a higher order effect and can be neglected. Moreover, the contribution to the scattered wave is integrated over the first Fresnel zone only. By definition, the scatters within the first zone radiate in phase with the background wave field, which indicates that the precise location of the scatters is of minor importance. The discrete distribution of the scatters within the layer can be replaced by a smooth scatter sheet density ν . In this letter, we use the result obtained in Ref. 17 and write the explicit form of the transmission coefficient T for the layer consisting of randomly distributed scatters in the weak scattering density limit:

$$T = \left(1 - i \frac{2\pi\nu}{k} f(k_i, k_i) \right). \quad (4)$$

In the MFSA approximation, the attenuation and dispersion of the transmitted/scattered waves is relatively insensitive to the shapes of the scatters as the forward scattering amplitude is relatively insensitive to the shape of the scatter.¹⁸ For any distribution $p(\alpha)$ in any number of parameters of the scatters, the forward scattering amplitude $f(k_i, k_i)$ be replaced by the average $\bar{f}(k_i, k_i)$ given by:

$$\bar{f}(k_i, k_i) = \int d\alpha p(\alpha) f(k_i, k_i); \alpha. \quad (5)$$

We carried out test numerical calculations for Si/Ge QDS and compared the results with experimental data. The experimental data have been obtained for two samples—A and B, grown by a solid source molecular beam epitaxy (MBE) system on Si (100) substrates. The growth started with a 100 nm Si buffer layer, followed by a quantum dot superlattice layer which is composed of bilayers in which the Ge layer is separated by a 20 nm Si spacer layer. Sample A consists of ten periods of dome-like Ge dots with 114.7 nm base, 15.1 nm height, a dot sheet density 5.9×10^8 dots per cm^{-2} , and a nominal Ge thickness 1.5 nm. Sample B consists of 22 periods of Ge dots with 152.4 nm base, 10.0 nm height, a dot sheet density 1.4×10^8 dots per cm^{-2} , and a nominal Ge thickness 1.2 nm. Thermal conductivity of the samples was measured by the differential 3ω method.¹⁹ The reference sample used for differential measurement is the same as the substrate used in the grown samples. In numerical simulations we used the procedure described above. First, we found the forward scattering amplitude assuming all dots be identical hemispheres of radius a , such as $1/3 d^2 H = 2/3 \pi a^3$, where d is the dot base size and H is the dot height. Then, we calculated reflection coefficient of a single quantum dot layer. Next, we found the total scattering cross section due to the scattering on quantum dots by summation of all scattered waves from all layers. Finally, we substituted the obtained attenuation length in Eq. (2). (The detailed calculations for other attenuation lengths in silicon can be found, for example, in Ref. 20.) The same procedure was repeated for different phonon frequencies and the lattice thermal conductivity was found by integration in Eq. (1). For both samples, the condition $|nf(k_i, k_i)/k^2| \ll 1$ is well met.

Figure 2 shows experimental data for samples A and B (plotted with markers) as well as results of numerical simu-

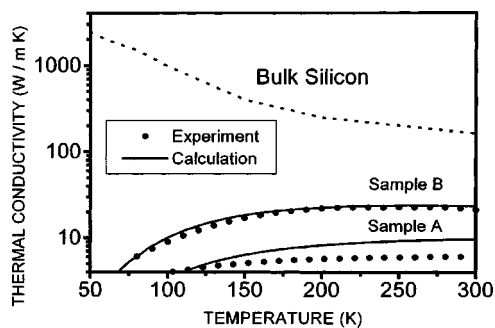


FIG. 2. Comparison between theoretical and experimental data. The markers depict experimental data obtained for SiGe QDS (samples A and B). Solid lines depict the results of numerical calculations. The dashed line depicts reference bulk silicon thermal conductivity.

lation (solid curves). The dashed line depicts reference bulk silicon thermal conductivity. The thermal conductivity is plotted as a function of temperature. It is clear that the temperature dependence of thermal conductivity trends as well as absolute values for both samples are in good agreement with the experimental data. The difference in deviation between theoretical and experimental data observed for samples A and B can be attributed to the higher order effects, as surface roughness, stress distribution in the quantum dot layer, which were not taken into consideration.

In conclusion, we present this theoretical model allowing us to estimate the cross-plane lattice thermal conductivity of semiconductor quantum dot superlattices. The agreement between the calculated and experimental data confirms our approach based on the continuum model approximation and the assumption that the thermal phonon wave can be represented by a sum of plane waves affected by the scattering on acoustically mismatched obstacles. The proposed calculation pro-

cedure is applicable in the most usual cases, where dot volume fraction is relatively small or dot and host materials have close acoustic properties.

The authors thank Professor G. Chen for valuable discussions. This work was, in part, supported by the AFOSR MURI Program on Phonon Control for Enhanced Device Performance (Dr. Dan Johnstone).

- ¹X. L. Lei and X. F. Wang, *Superlattices Microstruct.* **13**, 185 (1993).
- ²O. Lazarenkova and A. Balandin, *J. Appl. Phys.* **89**, 5509 (2001).
- ³D. L. Huffaker, G. Park, Z. Zou, O. B. Schekin, and D. G. Deppe, *Appl. Phys. Lett.* **73**, 2564 (1998).
- ⁴J. L. Liu, Y. S. Tang, K. L. Wang, T. Radetic, and R. Gronsky, *Appl. Phys. Lett.* **74**, 1863 (1999).
- ⁵T. C. Harman, P. J. Taylor, D. L. Spears, and M. P. Walsh, in *Abstracts of 41st Electronic Materials Conference*, Santa Barbara, (1999).
- ⁶A. Khitun, K. L. Wang, and G. Chen, *Nanotechnology* **11**, 327 (2000).
- ⁷S. Volz, J. B. Saulnier, G. Chen, and P. Beauchamp, *Microelectron. J.* **31**, 815 (2000).
- ⁸W. G. Wu, J. L. Liu, Y. S. Tang, G. L. Jin, and K. L. Wang, in *Proc. SPIE* **3630**, 98 (1999).
- ⁹J. L. Liu, W. G. Wu, A. Balandin, G. L. Jin, and K. L. Wang, *Appl. Phys. Lett.* **74**, 185 (1999).
- ¹⁰A. I. Yakimov, A. V. Dvurechenskii, V. V. Kirienko, Yu. I. Yakovlev, and A. I. Mikiforov, *Phys. Rev. B* **61**, 10868 (2000).
- ¹¹P. G. Klemens, in *Solid State Physics*, edited by F. Seitz and D. Turnbull (Academic, New York, 1958).
- ¹²G. P. Srivastava, *The Physics of Phonons* (Adam Hilger, New York, 1990).
- ¹³L. L. Foldy, *Phys. Rev.* **67**, 107 (1945).
- ¹⁴M. Lax, *Rev. Mod. Phys.* **23**, 287 (1951).
- ¹⁵P. C. Waterman and R. Truell, *J. Math. Phys.* **2**, 512 (1961).
- ¹⁶H. C. van der Hulst, *Physica (Amsterdam)* **15**, 740 (1949).
- ¹⁷J. Groenenboom and R. Snieder, *J. Acoust. Soc. Am.* **98**, 3482 (1995).
- ¹⁸C. F. Bohern and S. B. Singham, *J. Geophys. Res., [Atmos.]* **96**, 5269 (1991).
- ¹⁹S. M. Lee and D. G. Cahill, *J. Appl. Phys.* **81**, 2590 (1997).
- ²⁰A. Khitun, A. Balandin, and K. L. Wang, *Superlattices Microstruct.* **26**, 181 (1999).